

**Title:** Cyclotron produced  $^{132}\text{La}$  as a PET imaging surrogate of therapeutic  $^{225}\text{Ac}$

**Running title:**  $^{132}\text{La}/^{225}\text{Ac}$  theranostics

Eduardo Aluicio-Sarduy<sup>1</sup>, Todd E. Barnhart<sup>1</sup>, Jamey Weichert<sup>2</sup>, Reinier Hernandez<sup>1,2\*</sup> and Jonathan W. Engle<sup>1,2\*</sup>.

<sup>1</sup>Departments of Medical Physics, University of Wisconsin Madison

<sup>2</sup>Departments of Radiology, University of Wisconsin Madison

\*Co-corresponding authors: Jonathan W. Engle (Assistant Professor) and Reinier Hernandez, Department of Medical Physics and Department of Radiology, University of Wisconsin-Madison. 1111 Highland Avenue B1303 WIMR Cyclotron Laboratory, Madison WI 53705, USA.

Dr. Engle email: [jwengle@wisc.edu](mailto:jwengle@wisc.edu), tel: (608)-263-5805. Dr. Hernandez email: [hernandez6@wisc.edu](mailto:hernandez6@wisc.edu), tel: (305)-321-9806.

## ABSTRACT

The aim of this work is to explore  $^{132}\text{La}$  as a PET imaging surrogate of  $^{225}\text{Ac}$  using a DOTA-based, tumor-targeting alkylphosphocholine (NM600). **Methods:**  $^{132}\text{La}$  was produced on a biomedical cyclotron. For *in vivo* experiments, mice bearing 4T1 tumors were administered  $^{132}\text{La}$ -NM600, and PET/CT scans were acquired up to 24h post-injection (p.i.). Following the last timepoint, *ex vivo* tissue distribution was measured to corroborate *in vivo* PET data. *Ex vivo* tissue distribution was performed at 4h and 24h p.i. in mice injected with  $^{225}\text{Ac}$ -NM600. **Results:** PET/CT images showed elevated, persistent  $^{132}\text{La}$ -NM600 uptake in the tumor. Low bone accumulation confirmed the *in vivo* stability of the conjugate. *Ex vivo* biodistribution validated the image-derived quantitative data, and the comparison of the  $^{132}\text{La}$ -NM600 and  $^{225}\text{Ac}$ -NM600 tissue distribution

revealed similar biodistribution of the two radiotracers. **Conclusions:** These findings suggest that  $^{132}\text{La}$  is a suitable imaging surrogate to probe the *in vivo* biodistribution of  $^{225}\text{Ac}$  radiotherapeutics.

## KEYWORDS

Theranostics, PET, alpha-emitters, Actinium, Radiolanthanum.

## INTRODUCTION

Targeted Radionuclide Therapy (TRT) is a powerful systemic approach to cancer treatment. Recent clinical evidence demonstrates its potential to revolutionize the management of advanced-stage cancers (1,2). To date,  $^{225}\text{Ac}$  ( $T_{1/2} = 9.92$  d, 100%  $\alpha$ ,  $E_{\alpha} = 5.78$  MeV) is one of the most promising radionuclides for TRT (3). Its physical and chemical properties are suitable for the generation of radiopharmaceuticals based on small molecules, peptides, antibodies, and antibody fragments. Logistically, the long half-life of  $^{225}\text{Ac}$  enables centralized production and global distribution. However, the lack of isotopes of actinium with imageable emissions makes the noninvasive characterization of  $^{225}\text{Ac}$  pharmaceuticals' biodistribution difficult, and requires surrogate radiometals for imaging (2,4). Imaging of  $^{213}\text{Bi}$  ( $t_{1/2} = 43.59$ min, 97.80%  $\beta^{-}$ , 2.20%  $\alpha$ , 25.94% 440.45keV  $\gamma$ ),  $^{225}\text{Ac}$ 's third radioactive daughter, using SPECT has been proposed (5), but quantitation is difficult given the lack of radioactive equilibrium *in vivo*. Other radionuclides (e.g.,  $^{68}\text{Ga}$ ) with significant chemical dissimilarity to actinium are currently employed for this purpose, despite reports that the choice of radionuclide can affect the pharmacokinetics of radiopharmaceuticals (6). We and others hypothesize that lanthanum-labeled agents' biodistribution mirrors actinium agents' *in vivo* (7-9), but this hypothesis is yet to be tested. Our goal is to evaluate the potential of positron-emitting  $^{132}\text{La}$  ( $T_{1/2}=4.59$ h, 42%  $\beta^{+}$ ) as PET imaging surrogate of  $^{225}\text{Ac}$  with a well-characterized, tumor-targeting alkylphosphocholine (NM600)

developed by our group and used for TRT applications with  $^{90}\text{Y}$ ,  $^{177}\text{Lu}$ , and  $^{225}\text{Ac}$  (10-12). The compound has selective tumor uptake and retention in a wide variety of cancer types, including the murine mammary adenocarcinoma 4T1 model employed in this work.

## MATERIALS AND METHODS

All solutions were prepared using 18 M $\Omega$  cm $^{-1}$  water and optima grade HNO $_3$  and HCl from Fisher Chemical. The barium target material was acquired from Sigma-Aldrich (99.9%, trace metal basis) and stored in argon atmosphere. The synthesis of 2-(trimethylammonio)ethyl(18-(4-(2-(4,7,10-tris(carboxymethyl)-1,4,7,10-tetraazacyclododecan-1-yl)acetamido)phenyl)octadecyl) phosphate (NM600) has been described elsewhere (11).

### Radiochemistry and stability

Lanthanum-132 was produced by proton irradiation of metallic  $^{\text{nat}}\text{Ba}$  targets via the  $^{\text{nat}}\text{Ba}(p,n)^{132}\text{La}$  reaction on a 16 MeV GE PETtrace cyclotron (7). Irradiations of  $^{\text{nat}}\text{Ba}$  also produce the low-energy electron-emitting radionuclide  $^{135}\text{La}$  ( $t_{1/2} = 19.93\text{h}$ , 100%EC). Under these irradiation conditions (11.9MeV, 20 $\mu\text{A}$ , 3h), typical  $^{132}\text{La}$  and  $^{135}\text{La}$  decay corrected physical yields were 0.26 and 5.6 MBq  $\mu\text{A}^{-1}$ , respectively (7,8). Radiochemical isolation of  $^{132/135}\text{La}^{3+}$  ( $^{13x}\text{La}^{3+}$ ) was performed by precipitation and single-column extraction chromatography as previously described (7).  $^{225}\text{Ac}$  was obtained as  $^{225}\text{Ac}(\text{NO}_3)_3$  from Oak Ridge National Laboratory.

For radiolabeling of NM600 with  $^{13x}\text{La}$  or  $^{225}\text{Ac}$ , 340-370MBq of  $^{13x}\text{La}$  and 3.7MBq of  $^{225}\text{Ac}$  were mixed with NM600 (3.7MBq/nmol) in 0.1M NaOAc buffer solution (pH=5) at 80°C for 30 minutes under constant shaking (500 rpm). Complexes were purified by solid-phase extraction chromatography using Sep Pak C18 cartridges (Waters), eluted in absolute ethanol,

dried, and reformulated in phosphate-buffered solution (PBS) for injection.  $^{139}\text{La}$  or  $^{225}\text{Ac}$  activities were quantified by HPGe spectrometry (Al-windowed, Full-Width-Half-Maximum 1.8keV@1333 keV). The Radiochemical yield was assessed by thin-layer chromatography (TLC) using 50 mM ethylenediaminetetraacetic acid (EDTA) mobile phase. To assess stability,  $^{139}\text{La}$ -NM600 and  $^{225}\text{Ac}$ -NM600 complexes were incubated at 37°C in whole mouse serum, and samples were analyzed by TLC after 4 and 24h of incubation (n = 3).  $^{225}\text{Ac}$ -NM600 TLC samples were counted 4h after spotting the plates to ensure secular equilibrium conditions. Radiochemical purity and stability for the  $^{139}\text{La}$ -NM600 complex was confirmed via radio-high-performance liquid chromatography (HPLC) using a reverse-phase 250x3.00 mm C18 Luna 5 $\mu$  100A column (Phenomenex) and a water:acetonitrile gradient (5% MeCN:0-2 min; 5-65% MeCN:2-30 min; 65-90% MeCN:30-35min; 90-5% MeCN: 35-45 min).

### **PET/CT imaging and *ex vivo* biodistribution**

Murine mammary adenocarcinoma 4T1 cell lines were obtained from ATCC. The cells were cultured in completed media (RPMI-1640) supplemented with 10% FBS and 1% penicillin/streptomycin in an incubator at 37°C and 5% CO<sub>2</sub> atmosphere. All animal experiments were carried out under the approval of the University of Wisconsin Institutional Animal Care and Use Committee. Tumors were subcutaneously grafted injecting 5.0-7.5 $\times 10^5$  4T1 cells into the right lower flank of 6-8-week old female Balb/C mice (Envigo). Mice were employed for *in vivo* imaging and *ex vivo* biodistribution approximately two weeks after implantation, when tumor volume reached 400-600mm<sup>3</sup>.

For *in vivo* PET/CT imaging, mice were intravenously (IV) administered 3.7MBq of  $^{132}\text{La}$ -NM600 (30nmol) (n=3) in 200 $\mu$ L of phosphate-buffered saline (PBS). After isoflurane anesthesia

(2-4%), 40-80 million coincidence event PET scans (time window: 3.432ns, energy window: 350-650keV) were acquired at 4, 10, and 24h p.i. of the radiotracer. CT scans were performed prior to each PET acquisition for attenuation correction and anatomical co-registration. Quantitative region-of-interest (ROI) analysis of the PET images was carried out by manually drawing region-of-interest to quantify the radionuclide uptake in the tumor and healthy organs/tissues. Following the last imaging timepoint at 24 h p.i., *ex vivo* tissue distribution was measured to corroborate *in vivo* PET data and further examine the similarity between  $^{132}\text{La}$ -NM600 and  $^{225}\text{Ac}$ -NM600. *Ex vivo* tissue distribution was also performed at 4 and 24h p.i. in mice (n=3) injected IV with  $^{225}\text{Ac}$ -NM600 0.01MBq (0.003nmol) in 200 $\mu\text{L}$  of PBS. Mice were sacrificed by  $\text{CO}_2$  asphyxiation and tumor and other tissues were collected, wet-weighed, and counted in a calibrated automatic gamma counter (Wizard 2, Perkin Elmer).  $^{132}\text{La}$  was quantified using an energy window from 10 to 100keV.  $^{225}\text{Ac}$  samples were counted 4 h after organ harvesting to ensure secular equilibrium conditions using an energy window from 50 to 550keV. Quantitative data are reported as percent injected activity per gram of tissue (%IA/g  $\pm$  SD).

## RESULTS

### Radiochemistry and stability

Both  $^{132}\text{La}$ -NM600 and  $^{225}\text{Ac}$ -NM600 were produced in almost quantitative radiochemical yields (>95%) at a similar DOTA-based apparent molar activity of 3.7 MBq/nmol. The stability of both radio-conjugates was evaluated by radio-TLC up to 24h post-incubation. Stabilities >98% were observed, indicating minimal degradation of  $^{132}\text{La}$ -NM600 and  $^{225}\text{Ac}$ -NM600 in whole mouse serum (Figure 1A, Supplemental Table 1).

Radiochemical purity and serum stability of  $^{13x}\text{La-NM600}$  were corroborated by radio-HPLC (Figure 1B-C). A radio-peak (Rt: 26.04 min) corresponding to the  $^{13x}\text{La-NM600}$  complex was observed in all radio-chromatograms. Moreover, no additional radio-peaks were noted in either the solvent front (rt<3 min) or at different retention times, indicating the absence of “free”  $^{13x}\text{La}^{3+}$  or  $^{13x}\text{La-NM600}$  degradation products (Figure 1B). Similar results were observed after incubation of  $^{13x}\text{La-NM600}$  in mouse serum for 24h (Figure 1C).

### ***In vivo* imaging and *ex vivo* biodistribution**

Figure 2A shows representative maximum intensity projection (MIP) PET images after IV injection of  $^{132}\text{La-NM600}$  in balb/c mice bearing 4T1 tumors.  $^{132}\text{La-NM600}$  uptake in the tumor was elevated and persistent, reaching  $11.5\pm 1.3\% \text{IA/g}$  at 24h p.i. (Figure 2B, Supplemental Table 2). Blood pool activities were initially high ( $17.8\pm 1.3\% \text{IA/g}$ ) and gradually declined to  $13.8\pm 1.3$  and  $7.3\pm 0.8\% \text{IA/g}$  in the two later timepoints. Accumulation in liver peaked at  $18.3\pm 0.5\% \text{IA/g}$ , 10h p.i., and uptake in the kidneys was relatively low ( $<7\% \text{IA/g}$ ) at all imaging timepoints. Accumulation in other normal tissues and organs remained below  $5\% \text{IA/g}$ . These imaging results showed agreement with the  $^{225}\text{Ac-NM600}$  distributions obtained by *ex vivo* gamma counting (Figure 2B, Supplemental Table 3). Similarly, elevated blood ( $16.8\pm 0.8\% \text{IA/g}$ ) and liver uptake ( $11.9\pm 0.6\% \text{IA/g}$ ) were seen for  $^{225}\text{Ac-NM600}$  at 4 h p.i.. Blood values declined over the next 24h to  $5.7\pm 0.3\% \text{IA/g}$  and liver uptake increased to  $17.5\pm 0.3\% \text{IA/g}$ . An increase of  $^{225}\text{Ac-NM600}$  uptake in the tumor from  $4.6\pm 0.4\% \text{IA/g}$  to  $11.5\pm 2.1\% \text{IA/g}$  was also observed during the same period. *Ex vivo* biodistribution performed following the last PET/CT scan (Figure 3) confirmed the image-derived quantitative data showing elevated  $^{132}\text{La-NM600}$  uptake in the tumor ( $11.1\pm 0.8\% \text{IA/g}$ ), liver ( $17.0\pm 0.9\% \text{IA/g}$ ), and blood ( $9.9\pm 0.2\% \text{IA/g}$ ). A more extensive

comparison of  $^{132}\text{La}$ -NM600 and  $^{225}\text{Ac}$ -NM600 tissue distribution at 24h p.i. revealed effectively identical biodistribution of the two radiotracers.

## DISCUSSION

Lanthanides, and specifically  $\text{La}^{3+}$ , have been identified as suitable non-radioactive surrogates for  $\text{Ac}^{3+}$  (13). Chemical similarities between these two ions have been exploited to unravel the chemistry of actinium and stable lanthanum has been instrumental to the design of novel chelators that stably retain  $^{225}\text{Ac}$  *in vivo* (13). Although the potential of different radiolanthanums as PET imaging surrogate of  $^{225}\text{Ac}$  has been proposed (7-9), to date, no direct comparison between the *in vivo* distribution of a radioactive compound labeled to Ac or La has been performed. Thanks to a half-life of several hours, higher positron branching ratio and simpler, scalable production on low energy cyclotrons, we chose  $^{132}\text{La}$  from the unstable lanthanum radioisotopes with positron emissions. Coproduced  $^{135}\text{La}$  can be minimized with irradiation of isotopically enriched  $^{132}\text{Ba}$ , however, the results of the proof-of-concept imaging studies reported herein are not affected by the presence of  $^{135}\text{La}$ .

Our observed *in vitro* stability of  $^{132}\text{La}$ -NM600 and  $^{225}\text{Ac}$ -NM600 is in agreement with previously reported for DOTA compounds with  $^{225}\text{Ac}$  and  $^{140}\text{La}$ , showing that both DOTA complexes were stable for several days after incubation in human or complete mouse serum (12,14). High tumor uptake *in vivo* and *ex vivo* confirms the tumor-selectivity of the targeting vector. Hepatobiliary excretion of the tracer is also apparent. The observed low bone accumulation is indicative of the *in vivo* stability of the  $^{132}\text{La}$ -NM600 radioconjugate –“free” radiolanthanum has been shown to lodge in the bones in mice (7). *Ex vivo* biodistribution analysis further validates the image-derived quantitative data and the similar  $^{132}\text{La}$ -NM600 and  $^{225}\text{Ac}$ -NM600 tissue

distribution support the hypothesis that  $^{132}\text{La}$  is a suitable imaging surrogate of  $^{225}\text{Ac}$  targeted radiotherapeutic drugs *in vivo*.

One limitation of  $^{132}\text{La}$  is its 4.59h half-life compared to the 9.92d of  $^{225}\text{Ac}$ . This difference is not critical for fast clearing small molecules such as PSMA, FAPI, DOTATATE, among many others clinically relevant small biomolecules. However, in the case of macromolecules with longer biological half-lives such as antibodies and antibody derivatives,  $^{132}\text{La}$  will likely not be suitable for protracted imaging timepoint. Nonetheless, evidence suggests that the effects of the radioisotope's chemical properties on the pharmacokinetic profile of these compounds is less pronounced, in which case other trivalent imaging surrogates like  $^{86}\text{Y}^{3+}$  and  $^{111}\text{In}^{3+}$  may be appropriate (11,15).

## CONCLUSIONS

This work demonstrates the potential of  $^{132}\text{La}$  as PET imaging surrogate to probe the *in vivo* biodistribution of  $^{225}\text{Ac}$  radiotherapeutics. Our results warrant future development of the theranostic  $^{132}\text{La}/^{225}\text{Ac}$  pair, which will require isotopically enriched  $^{132}\text{Ba}$  targets to produce larger quantities of highly pure  $^{132}\text{La}$ .



## DISCLOSURE

J.P.W. is the founder and CSO of Archeus Technologies Inc. who has licensing rights to NM600. J.P.W. and R.H. have an equity stake in Archeus Technologies Inc. The authors declare that no other competing interest exists.

## ACKNOWLEDGEMENTS

We are grateful to Archeus Technologies Inc. for providing the NM600 precursor. We thank the staff of the UW Small Animal Imaging Facility and the University of Wisconsin Carbone Cancer Center for their support. EAS gratefully acknowledges the financial support from the National Institutes of Health under Award Number T32CA009206.

## KEY POINTS

**Question:** Is the positron-emitter  $^{132}\text{La}$  a suitable PET imaging surrogate to probe the *in vivo* biodistribution of  $^{225}\text{Ac}$  radiotherapeutics?

**Pertinent findings:**  $^{132}\text{La}$  PET image-derived and *ex vivo* pharmacokinetics match the measured biodistribution of  $^{225}\text{Ac}$  in a murine model of breast cancer, targeted with a DOTA-based small molecule (NM600) throughout the usual lifetime of  $^{132}\text{La}$ .

**Implications for patient care:** These findings and the straightforward cyclotron production of positron-emitting  $^{132}\text{La}$  make it an attractive candidate for rapid, non-invasive screening of  $^{225}\text{Ac}$  radiopharmaceuticals.

## REFERENCES

1. Kratochwil C, Bruchertseifer F, Giesel FL, et al.  $^{225}\text{Ac}$ -PSMA-617 for PSMA-Targeted  $\alpha$ -Radiation Therapy of Metastatic Castration-Resistant Prostate Cancer. *J Nucl Med* . 2016;57:1941-1944.
2. Sathekge M, Bruchertseifer F, Vorster M, et al. Predictors of Overall and Disease-Free Survival in Metastatic Castration-Resistant Prostate Cancer Patients Receiving  $^{225}\text{Ac}$ -PSMA-617 Radioligand Therapy. *J Nucl Med* . 2020;61:62-69.
3. Morgenstern A, Apostolidis C, Kratochwil C, Sathekge M, Krolicki L, Bruchertseifer F. An Overview of Targeted Alpha Therapy with  $(^{225})\text{Actinium}$  and  $(^{213})\text{Bismuth}$ . *Curr Radiopharm*. 2018;11:200-208.
4. Lenzo NP, Meyrick D, Turner JH. Review of Gallium-68 PSMA PET/CT Imaging in the Management of Prostate Cancer. *Diagnostics (Basel, Switzerland)*. 2018;8:16.
5. de Swart J, Chan HS, Goorden MC, et al. Utilizing High-Energy  $\gamma$ -Photons for High-Resolution  $^{213}\text{Bi}$  SPECT in Mice. *J Nucl Med* . 2016;57:486-492.
6. Hernandez R, Aluicio-Sarduy E, Grudzinski J, Pinchuk A, Engle J, Weichert J. Choice of radiometal influences the tumor targeting and biodistribution properties of theranostic alkylphosphocholine chelates *in vivo*. *J Nucl Med* . 2018;59:533.
7. Aluicio-Sarduy E, Hernandez R, Olson AP, et al. Production and *in vivo* PET/CT imaging of the theranostic pair  $^{132/135}\text{La}$ . *Sci Rep*. 2019;9.
8. Aluicio-Sarduy E, Thiele NA, Martin KE, et al. Establishing Radiolanthanum Chemistry

- for Targeted Nuclear Medicine Applications. *Chem – A Eur J.* 2020;26:1238-1242.
9. Bailey T, Lakes A, An D, Gauny S, Abergel R. Biodistribution Studies of Chelated Ce-134/La-134 as Positron-Emitting Analogues of Alpha-Emitting Therapy Radionuclides. *J Nucl Med.* 2019;60:130-130.
  10. Hernandez R, Walker KL, Grudzinski JJ, et al. <sup>90</sup>Y-NM600 targeted radionuclide therapy induces immunologic memory in syngeneic models of T-cell Non-Hodgkin's Lymphoma. *Commun Biol.* 2019;2:79.
  11. Hernandez R, Grudzinski JJ, Aluicio-Sarduy E, et al. <sup>177</sup>Lu-NM600 targeted radionuclide therapy extends survival in syngeneic murine models of triple-negative breast cancer. *J Nucl Med.* December 2019:jnumed.119.236265.
  12. Hernandez R, Aluicio-Sarduy E, Grudzinski J, et al. <sup>225</sup>Ac-NM600 Targeted Alpha Therapy Extends Survival in a Model of Triple Negative Breast Cancer. *J Med Imaging Radiat Sci.* 2019;50:S35.
  13. Thiele NA, Brown V, Kelly JM, et al. An Eighteen-Membered Macrocyclic Ligand for Actinium-225 Targeted Alpha Therapy. *Angew Chemie Int Ed.* 2017;56:14712-14717.
  14. Li WP, Ma DS, Higginbotham C, et al. Development of an in vitro model for assessing the in vivo stability of lanthanide chelates. *Nucl Med Biol.* 2001;28:145-154.
  15. Kelly VJ, Wu S-T, Gottumukkala V, et al. Preclinical evaluation of an <sup>111</sup>In/<sup>225</sup>Ac theranostic targeting transformed MUC1 for triple negative breast cancer. *Theranostics.* 2020;10:6946-6958.

## FIGURES

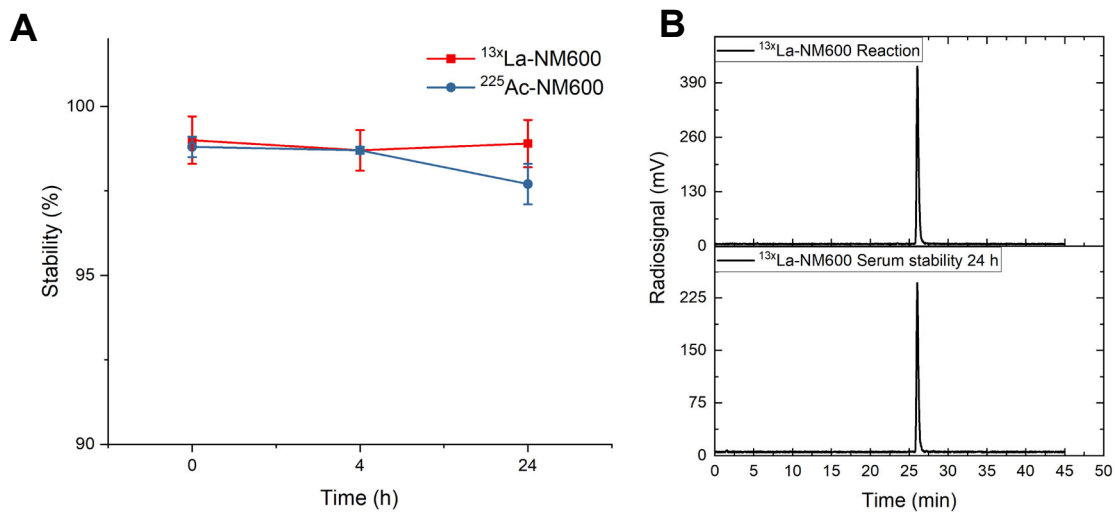


**Figure 1.** (A)  $^{13}\text{xLa-NM600}$  and  $^{225}\text{Ac-NM600}$  mouse serum stability quantified by r-TLC (n=3, mean $\pm$ SD) (B) Radio-HPLC chromatogram of the  $^{13}\text{xLa-NM600}$  radiolabeling reaction (3.7MBq/nmol) after an incubation time of 30min (C)  $^{13}\text{xLa-NM600}$  serum stability chromatogram at 24h post-incubation.

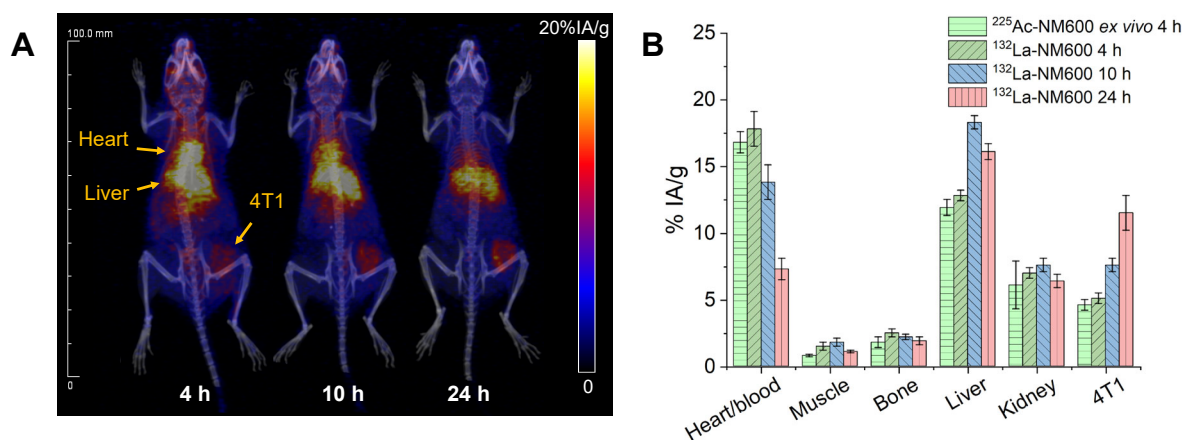


**Figure 2.** (A) Maximum intensity projection (MIP) static PET images of a representative balb/c mouse injected intravenously with  $^{132}\text{La-NM600}$ . (B)  $^{132}\text{La-NM600}$  tissue uptake quantification of PET ROIs in mice (n=3, mean $\pm$ SD) injected with  $^{132}\text{La-NM600}$ . *Ex vivo*  $^{225}\text{Ac-NM600}$  biodistribution data at 4h are also included for comparison.

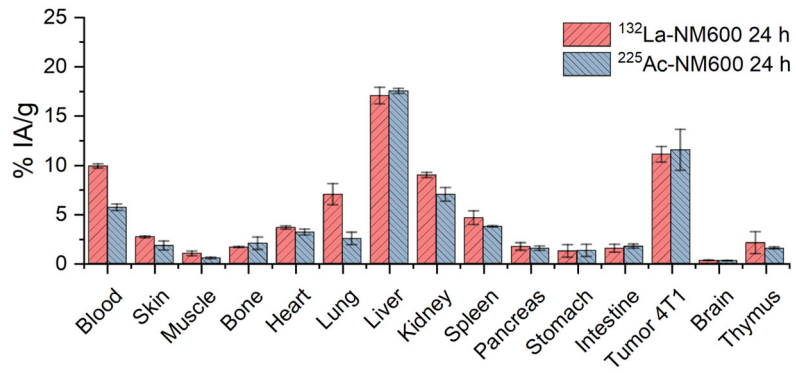


**Figure 3.** *Ex vivo*  $^{132}\text{La-NM600}$  and  $^{225}\text{Ac-NM600}$  biodistribution at 24 h p.i., measured by gamma counting (n = 3, mean  $\pm$  SD).

Graphical Abstract:

